BRAF^{V600E} mutation, TIMP-1 upregulation, and NF-κB activation: closing the loop on the papillary thyroid cancer trilogy

Alessandra Bommarito[1], Pierina Richiusa[1], Elvira Carissimi[1], Giuseppe Pizzolanti[1], Vito Rodolico[3], Giovanni Zito[1], Angela Criscimanna[1], Francesco Di Blasi[2], Maria Pitrone[1], Monica Zerilli[3], Marco C Amato[1], Gaetano Spinelli[2], Valeria Carina[1], Giuseppe Modica[4], M Adelfio Latteri[5], Aldo Galluzzo[1] and Carla Giordano[1,2]

[1]Sezione di Endocrinologia, Laboratorio di Endocrinologia Molecolare, Dipartimento di Biomedico di Medicina Interna e Specialistica (DIBIMIS), University of Palermo, 90127 Palermo, Italy
[2]CNR-IBIM, Institute of Biomedicine and Molecular Immunology, 90146 Palermo, Italy
[3]Istituto di Anatomia Patologica, [4]Sezione di Chirurgia Generale ad Indirizzo Toracico, Dipartimento di Discipline Chirurgiche ed Oncologiche and [5]Chirurgia Oncologica, University of Palermo, 90127 Palermo, Italy

(Correspondence should be addressed to C Giordano at Sezione di Endocrinologia, Laboratorio di Endocrinologia Molecolare, Dipartimento di Biomedico di Medicina Interna e Specialistica (DIBIMIS), University of Palermo; Email: cgiordan@unipa.it)

Abstract

BRAF^{V600E} is the most common mutation found in papillary thyroid carcinoma (PTC). Tissue inhibitor of metalloproteinases (TIMP-1) and nuclear factor (NF)-κB have been shown to play an important role in thyroid cancer. In particular, TIMP-1 binds its receptor CD63 on cell surface membrane and activates Akt signaling pathway, which is eventually responsible for its anti-apoptotic activity. The aim of our study was to evaluate whether interplay among these three factors exists and exerts a functional role in PTCs. To this purpose, 56 PTC specimens were analyzed for *BRAF*^{V600E} mutation, TIMP-1 expression, and NF-κB activation. We found that *BRAF*^{V600E} mutation occurs selectively in PTC nodules and is associated with hyperactivation of NF-κB and upregulation of both TIMP-1 and its receptor CD63. To assess the functional relationship among these factors, we first silenced *BRAF* gene in BCPAP cells, harboring *BRAF*^{V600E} mutation. We found that silencing causes a marked decrease in *TIMP-1* expression and NF-κB binding activity, as well as decreased invasiveness. After treatment with specific inhibitors of MAPK pathway, we found that only sorafenib was able to increase IκB-α and reduce both *TIMP-1* expression and Akt phosphorylation in BCPAP cells, indicating that BRAF^{V600E} activates NF-κB and this pathway is MEK-independent. Taken together, our findings demonstrate that BRAF^{V600E} causes upregulation of TIMP-1 via NF-κB. TIMP-1 binds then its surface receptor CD63, leading eventually to Akt activation, which in turn confers antiapoptotic behavior and promotion of cell invasion. The recognition of this functional trilogy provides insight on how BRAF^{V600E} determines cancer initiation, progression, and invasiveness in PTC, also identifying new therapeutic targets for the treatment of highly aggressive forms.

Endocrine-Related Cancer (2011) **18** 669–685

Introduction

Thyroid cancer accounts for <1% of all new malignancies, although the occult form can be found in 5–36% of well-differentiated tumors of the thyroid gland (Schlumberger 1998, Davies & Welch 2006). Differentiated thyroid tumors include papillary thyroid carcinoma (PTC) and follicular thyroid carcinoma (FTC), which globally account for more than 80% of all forms (Leenhardt *et al*. 2004, Fontaine *et al*. 2009). The biological behavior of PTC varies widely, from indolent microcarcinomas, growing slowly with little or no invasion, to invasive tumors that metastasize and cause death. Nevertheless, the small size of the primary tumor is not necessarily related to lower malignant

1351–0088/11/018–669 © 2011 Society for Endocrinology *Printed in Great Britain*
DOI: 10.1530/ERC-11-0076
Online version via http://www.endocrinology-journals.org

potential, as about 10% of PTC patients die from distant metastases, which may appear several years after diagnosis (Hundahl *et al*. 1998, Cooper *et al*. 2006, Xing 2007).

The molecular mechanisms regulating initiation, progression, and invasiveness of PTC have not been fully elucidated. The RET/PTC-RAS-BRAF-MEK-ERK pathway (mitogen-activated protein kinase pathway or MAPK), which plays a fundamental role in several cell functions such as proliferation, differentiation, apoptosis, and survival, has been indicated as a key intracellular signaling pathway involved in thyroid carcinogenesis (Xing 2007). In particular, BRAF T1799A transversion has been described as the most frequent genetic alteration (Garnett & Marais 2004, Dhomen & Marais 2007). This mutation characterized by a V600E amino acidic change in the BRAF protein ($BRAF^{V600E}$), results in constitutive activation of BRAF (Davies *et al*. 2002, Wan *et al*. 2004) and has been associated with aggressive PTC subtypes (Xing 2007). $BRAF^{V600E}$ has been reported to be responsible for both the initiation of tumorigenesis and its progression. PTC metastatic lesions in lymph nodes harboring $BRAF^{V600E}$ have been described as larger in size than those harboring wild-type alleles ($BRAF^{WT}$; Rodolico *et al*. 2007).

Nuclear factor (NF)-κB has been also reported to play an important role in thyroid cancer (Visconti *et al*. 1997, Pacifico & Leonardi 2010). Recently, it has been hypothesized that $BRAF^{V600E}$ promotes invasiveness of thyroid cancer cells via NF-κB activation (Karin 2006, Palona *et al*. 2006), leading to acquisition of apoptotic resistance, although the mechanism has not been fully defined.

Metalloproteinases (MMPs) play a central role in tissue invasion, as they degrade extracellular matrices. MMPs are tightly regulated by specific inhibitors (tissue inhibitor of metalloproteinases, TIMPs), which control their activation in both physiological and pathological conditions (Sounni & Noel 2005, Deryugina & Quigley 2006). The TIMP-1 gene has been reported to be upregulated in thyroid tumors (Griffith *et al*. 2006). Specifically, increased expression of TIMP-1 has been identified as a candidate molecular biomarker for PTC (Hawthorn *et al*. 2004). Notably, in other tumors TIMP-1 is thought to exert functions that are independent of MMP inhibition, such as stimulation of proliferation and inhibition of apoptosis (Stetler-Stevenson 2008). Recently, TWIST1 was identified as an important regulation factor responsible for the expression of TIMP-1 (Okamura *et al*. 2009).

The aim of our study was therefore to evaluate whether interplay among $BRAF^{V600E}$, NF-κB, and TIMP-1 exists and exerts a functional role in PTCs. In this study, we demonstrate that $BRAF^{V600E}$ mutation, NF-κB activation, and TIMP-1 upregulation act as a trilogy which might explain the initiation, progression, and invasiveness of PTC.

Materials and methods

Tissue specimens

Fifty-six PTC specimens collected after patients' informed consent for the Sicilian Registry of Thyroid Tumors were retrospectively selected and used for this study. For each case, tissue from the tumoral nodule and the contralateral healthy lobe was analyzed for $BRAF^{V600E}$ mutation. We then selected 28 cases harboring $BRAF^{V600E}$ mutation and 28 $BRAF^{WT}$ based on matched age, gender distribution, and macroscopic characteristics. Clinical and histological characteristics with pTNM staging of selected PTCs are shown in Table 1. $BRAF^{V600E}$ was found in 22/28 classical variant (78.6%), 2/16 follicular variant (12.5%), 2/4 tall cell variant (50%), and 2/8 sclerosant variant (25%). $BRAF^{V600E}$ mutation was never detected in the contralateral healthy lobe. Correlation with prognosis was not available because the follow-up was <2 years. The IRB of the University of Palermo, Italy, approved the study.

Immunohistochemistry

All 56 primary lesions and the respective contralateral healthy lobes were analyzed. Briefly, 5 μm paraffin-embedded sections were deparaffinized, rehydrated, and microwave-heated in 10 mM sodium citrate buffer for antigen retrieval. Sections were then incubated with 3% hydrogen peroxide/PBS for 5 min, and blocked with 3% PBS/BSA. Incubation with mouse anti-human TIMP-1 antibody (MP Biomedical, DBA Italia, Milan, Italy, cat. 631661), mouse anti-human CD63 (Santa Cruz Biotechnology, DBA Italia, Milan, Italy, sc-5275), mouse anti-Bcl-2 IgG_1 (Santa Cruz Biotechnology, sc-7382), and rabbit anti-Bcl-xL (Santa Cruz Biotechnology, sc-1041) was performed at room temperature (RT) for 1 h. To detect specific expression, secondary biotinylated antibodies, streptavidin/HRP, and chromogen 3-amino-9-ethylcarbazole substrate were used. Counterstaining of cells and tissue sections was performed by aqueous hematoxylin. Images were acquired on a Zeiss Imager Z1 microscope with a Zeiss AxioCam driven by Zeiss AxioVision Rel.4.7 software. For quantification analysis, cells were counted using the Cell Counter Plugin of ImageJ software (http://rsb.info.nih.gov/ij/plugins/cell-counter.html).

Table 1 Clinical and histological characteristics of papillary thyroid carcinomas (no. 56) evaluated

	Wild type (no. 28) mean ± S.D.	Mutant (no. 28) mean ± S.D.	*P*
Age	45.07 ± 12.4	45.7 ± 16.36	0.897
	No. (%)	No. (%)	
Sex			0.121
Male	10 (35.7)	4 (14.3)	
Female	18 (64.3)	24 (85.7)	
Tumor size (T)[a]			0.350
T1a	8 (28.6)	14 (50)	
T1b	12 (42.8)	8 (28.6)	
T2	2 (7.14)	2 (7.14)	
T3	4 (14.3)	4 (14.3)	
T4	2 (7.14)	0 (0)	
Lymph node[a] metastasis			0.237
NX	10 (35.7)	12 (42.8)	
N0	16 (57.1)	10 (35.7)	
N1a	2 (7.14)	4 (14.3)	
N1b	0 (0)	2 (7.14)	
Metastasis[a]			0.771
Mx	5 (17.8)	6 (21.4)	
M0	22 (78.6)	20 (71.4)	
M1	1 (3.6)	2 (7.1)	
Multifocality			0.782
Present	10 (35.7)	11 (39.3)	
Sclerosis			0.192
Present	1 (3.6)	5 (17.8)	
Encapsulation			0.163
Present	13 (46.4)	7 (25)	
Histological variants			<0.001*
Classical	6 (21.4)*	22 (78.6)*	
Follicular	14 (50)	2 (7.14)	
Tall cell	2 (7.14)	2 (7.14)	
Sclerosant	6 (21.4)	2 (7.14)	

[a]TNM was assessed in accordance with AJCC/UICC TNM, 7th edition (2009). *, statistically significant value.

Positive and negative stained nuclei were marked placing different color marks by mouse clicking directly from the screen. For each case a minimum of 10^3 cells was counted, and the percentage of tumor cells stained with TIMP-1, CD63, Bcl-2, and Bcl-xL antibodies was regarded as labeling index (LI; Hsu *et al*. 2003). Only epithelial cells were counted regardless of intensity of staining. Twenty random cases were evaluated separately by two different observers (V R and M Z); since the variation was <5%, the first pathologist's data were used.

RNA extraction, RT-PCR, and qRT-PCR

All 56 primary lesions and the respective contralateral healthy lobes were analyzed. RNA was extracted using RNeasy Mini Kit (Qiagen, Milan, Italy) and was reverse transcribed with Oligo-dT primers (Applied Biosystems, Monza, Italy) and Stratascript RT (Stratagene, Amsterdam, The Netherlands), according to the manufacturer's protocol. Gene expression was analyzed by real-time quantitative PCR (qRT-PCR) with Quantitect SYBR Green PCR Kit (Qiagen) using a LightCycler 1.5 Instrument (Roche Diagnostics). Reactions were performed at least in triplicate. The specificity of the amplified products was determined by melting peak analysis. Quantification for each gene of interest was performed in relation to the appropriate standard curve. Gene expression was normalized against the housekeeping gene *β-actin*, which was stable among all the samples. PCR primers for *TIMP-1*, *TWIST1*, and *BRAF* were purchased from Qiagen (Quantitect Primer Assay, Hs_TIMP-1_SG, QT00084168; Hs_TWIST1_SG, QT00011956; Hs_BRAF_1_SG, QT00078176) while *β-actin* primers were purchased from Realtimeprimers.com. The PCR thermal cycler conditions were 95 °C for 15 min followed by 45 cycles of 95 °C for 15 s, 55 °C for 15 s, and 72 °C for 15 s.

Oligonucleotide microarray analysis

The expression profile of 113 genes was analyzed by the OligoGEArray Human Cancer PathwayFinderT microarray (Superarray Bioscience Corporation, Frederick, MD, USA) in 12 primary lesions and the respective contralateral healthy lobes. Briefly, 3 μg total RNA was used as a template, the cRNA probes were hybridized to Cancer GEArray DNA Microarray membrane overnight at 60 °C, and membranes were analyzed using GEArray Expression Analysis Suite.

DNA extraction and detection of *BRAF*^{V600E} mutation

BRAF^{V600E} mutation was detected in all 56 primary lesions and the respective contralateral healthy lobes by real-time allele-specific amplification as described previously (Pizzolanti *et al*. 2007). DNA was extracted and purified using Qiagen DNAeasy Tissue Kit, according to the manufacturer's protocol (Qiagen). DNA quantity and quality was assessed by u.v. spectrophotometry. Sequencing and Mutector assay (TrimGen, Milan, Italy) confirmed the allele-specificity of *BRAF*^{V600E} mutation (Pizzolanti *et al*. 2007).

Protein extraction and western blot analysis

Proteins were extracted from 32 samples (16 nodules and 16 healthy counterparts) and thyroid tumor cell lines using RadioImmunoPrecipitation Assay buffer

(50 mM Tris–HCl, pH 7.4, 150 mM NaCl, 1% Nonidet P40), supplemented with protease inhibitor cocktail (Complete mini, Roche) and phosphatase inhibitors. For cytosolic and nuclear protein extraction, two buffers were used: lysis buffer (NaCl 150 mM, Tris–HCl, pH 7.8, 0.01 M, $MgCl_2$ 1.15 mM, NP-40 0.65%, supplemented with protease inhibitor cocktail and phosphatase inhibitors) and nuclear extraction buffer (NaCl 0.15 M, Tris–HCl, pH 8, 50 mM, NP-40 1%, DOC 0.5%, SDS 0.1%, supplemented with protease inhibitor cocktail and phosphatase inhibitors). Protein content was determined according to Bradford's method.

Proteins were separated by NuPAGE 4–12% Bis-Tris Gel (Invitrogen), electrotransferred to nitrocellulose membranes, and blotted with the following primary antibodies: mouse antihuman TIMP-1 (MP Biomedical, cat. 631661), mouse anti-Raf-B F-7 IgG2a (Santa Cruz Biotechnology, sc-5284), rabbit anti-p-Akt1/2/3 Thr 308 (Santa Cruz Biotechnology, sc-16646-R), rabbit anti-Akt1/2/3 H-136 (Santa Cruz Biotechnology, sc-8312), goat anti-p-MEK-1/2 (Ser 218/Ser 222) (Santa Cruz Biotechnology, sc-7995), rabbit anti-MEK-1/2 (12-B) (Santa Cruz Biotechnology, sc-436), mouse anti-NFκB p65 (F-6) (Santa Cruz Biotechnology, sc-8008), mouse anti-IκB-α (6A920) (Santa Cruz Biotechnology, sc-56710), mouse anti-histone H2A (Upstate Millipore, Milan, Italy, cat. 07-146), mouse anti-Bcl-2 IgG_1 (Santa Cruz Biotechnology, sc-7382), rabbit anti-Bcl-xL (Santa Cruz Biotechnology, sc-1041), and mouse anti-β-actin IgG1 (Sigma–Aldrich, A5441). Secondary antibodies: goat anti-rabbit IgG-HRP (Santa Cruz Biotechnology, sc-2030) goat anti-mouse IgG-HRP (Santa Cruz Biotechnology, sc-2031) and donkey anti-goat IgG-HRP (Santa Cruz Biotechnology, sc-2033). Antigen–antibody complexes were visualized using SuperSignal West Femto Maximum Sensitivity Substrate (Thermo Fisher Scientific, Milan, Italy) on a CCD camera (Chemidoc, Bio-Rad). Western blot bands were quantified with Quantity One software (Bio-Rad).

Gelatin zymography for MMP-9

Electrophoresis of 50 μg proteins was performed on 7.5% polyacrylamide gels containing gelatine (2 mg/ml; Difco Lab, Milan, Italy) in 32 primary lesions and their healthy counterparts tissues as described previously (La Rocca *et al*. 2004). Gels were rinsed twice in 2.5% Triton-X100, and incubated at 37 °C for 20 h in a buffer containing 0.2 M NaCl, 5 mM $CaCl_2$, 50 mM Tris–HCl (pH 7.6), and 0.02% Briji-35 (Sigma–Aldrich). Gels were stained with 0.25% Coomassie blue and de-stained in 25% methanol and 10% acetic acid.

Electrophoretic mobility shift assay

Twenty microgram of total proteins from 32 samples (16 nodules and 16 respective contralateral healthy lobes) were incubated with a double-stranded ^{32}P-labeled oligonucleotide probe containing the specific recognition sequence for NF-κB (5′-AGTTGAGGGGACTTTC-CCAGGC-3′), as described previously (Kitchener *et al*. 2004). In addition, an unlabeled oligonucleotide was added in excess (100:1) to the labeled NF-κB probe, when appropriate for specific detection.

Cell cultures

Well-recognized human thyroid cell lines (Schweppe *et al*. 2008) harboring or not harboring $BRAF^{V600E}$ mutation were used for *in vitro* experiments. BCPAP ($BRAF^{V600E/V600E}$) and TPC-1 ($BRAF^{WT/WT}$) cell lines were cultured in RPMI 1640 medium supplemented with 10% FBS, 5% penicillin–streptomycin, and 5% glutamine. KTC-1 ($BRAF^{V600E/WT}$) cell line was cultured in DMEM supplemented with 5% FBS, 5% penicillin–streptomycin, and 5% glutamine. Cultures were maintained in 5% CO_2 at 37 °C in a humidified incubator.

Small interfering RNA transfection

Small interfering RNAs (siRNAs) were introduced into BCPAP cells using Interferin transfection agent (EuroClone, Milan, Italy), according to the manufacturer's instructions. Briefly, cells were seeded into six-well plates at a density of 300 000 cells/well or 96-well plates at a density of 7000 cells/well. Transfection agent and siRNA complex were added to cells and incubated for 48 and 72 h. Final concentration of siRNA was 100 nM. Each assay was performed in triplicate in at least five independent experiments. *TIMP-1* was silenced using On target Plus Smart Pool Timp-1 siRNA (L-011792-00, Dharmacon, Lafayette, CO, USA). *BRAF* was silenced using a chemically synthesized siRNA targeting $BRAF^{V600E}$ mutation (MU-A), as described previously (Hingorani *et al*. 2003). siCONTROL, non-targeting siRNA pool was used as a control (D-001206-13, Dharmacon).

Treatment with MAPK inhibitors

BCPAP cells were treated with 5 μM sorafenib (LKT Laboratories, Alexis Corporation, Lausen, Switzerland) and 3 μM U0126 (662005, Calbiochem, DBA Italia, Milan, Italy) up to 4 h. p-MEK, MEK, p-AKT, AKT, p65, IκB-α, and histone H2A expression was evaluated by western blot as described above. *TIMP-1* expression was evaluated by real-time PCR after 24 h of treatment.

Flow cytometry

Cells were incubated at RT for 30 min with mouse anti-human CD63 (Santa Cruz Biotechnology, sc-5275). After two washing steps with PBS, cells were incubated with goat anti-mouse IgG $F(ab)_2$ FITC (Santa Cruz Biotechnology, sc-3699). Cells were fixed with 4% paraformaldehyde for 10 min at RT and then resuspended in permeabilization buffer containing 0.1% (w/v) saponin, 0.05% (w/v) NaN3 in Hanks' balanced salt solution (HBSS). Cells were then incubated at RT for 30 min with PE-labeled monoclonal antibody for TIMP-1 (R&D Systems, Space Import-Export srl, Milan, Italy, IC970P, clone 635115). A negative control with an isotype-matched antibody was included. Cells were analyzed on a FACSCalibur flow cytometer (BD Biosciences, Milan, Italy), using CellQuest software (Becton and Dickinson, Milan, Italy).

Inhibition of NF-κB

BCPAP cells were plated in a six-well plate in 2 ml RPMI, stimulated for 24 h with 5 μM MG-132, 50 nM dexamethasone 21-phosphate (Sigma–Aldrich) and 10 μM parthenolide (sc-3523, Santa Cruz Biotechnology). Cells were then cultured for another 24 h with 30 μM monensin.

Immunofluorescence

Cells were cultured in culture-slides (BD Biosciences), and treated with 10 μM parthenolide for 24 h and subsequently for another 4 h with 30 μM monensin. Cells were fixed for 15 min at RT in 2% (wt/vol) paraformaldehyde, permeabilized, washed and blocked for 30 min with buffer containing 0.05% (w/v) saponin, and PBS/5% BSA (Sigma–Aldrich). Mouse monoclonal CD63 (Santa Cruz Biotechnology, sc-5275) was incubated for 1 h at RT and rabbit polyclonal TIMP-1 (H-150; Santa Cruz Biotechnology, sc-5538) for 24 h at 4 °C. Secondary antibodies (goat anti-rabbit IgG (H+L), Alexa Fluor 488, cat. A11008; chicken anti-mouse IgG (H+L), Alexa Fluor 594, cat. A21201, Invitrogen) were incubated for 1 h at RT. Images were acquired with TCS SP5 confocal microscope (Leica Microsystems).

Treatment with recombinant TIMP-1

BCPAP cells were plated in six-well plates in 2 ml serum-free medium/well for 24 h and then incubated with 250 ng/ml recombinant TIMP-1 protein (Calbiochem, PR019) for 30 and 60 min. Western blot for Akt, p-Akt, Bcl-2, and Bcl-xL was performed as described in the previous section.

BCPAP cells were plated in a 96-well plate in 100 μl serum-free medium/well and incubated with recombinant TIMP-1 protein up to 24 h at different concentrations (5–250 ng/ml). Cell proliferation was assessed by colorimetric assay using BrdU kit (Roche Diagnostics). BCPAP cells were also treated with 250 ng/ml of recombinant TIMP-1 protein (Calbiochem, PR019) up to 24 h to perform an invasion assay using BD BioCoat Matrigel invasion chambers (BD Biosciences).

Treatment with Akt inhibitor

BCPAP cells were treated with 10 μM Akt inhibitor VIII, Isozyme-Selective, Akti-1/2 (Calbiochem, 124018) for 4 h and p-Akt and Akt were evaluated by western blot. In addition, for evaluation of cell proliferation after Akt inhibition, BCPAP cells were incubated at 37 °C for 24 h with 10 μM Akt inhibitor. Cell proliferation was assessed by colorimetric assay using BrdU kit (Roche Diagnostics). BCPAP cells were also treated with 10 μM Akt inhibitor to perform an invasion assay using BD BioCoat Matrigel invasion chambers (BD Biosciences).

Invasion assay

BD BioCoat Matrigel invasion chambers (BD Biosciences) were rehydrated just before the assay using FBS-free RPMI according to the manufacturer's instructions. Cells were then resuspended in RPMI containing 0.1% BSA and 5×10^5 cells/0.5 ml cells were added to the invasion chamber. Inserts were transferred into the wells of a 24-well plate with 750 μl culture medium containing 5% FBS as a chemoattractant. The assembled chambers were incubated for 24 h at 37 °C. Non-migrating cells, which remained on the upper surface of the filter, were completely removed by wiping with a cotton swab. Cells on the underside of the insert were stained with 2.5 μg/ml of Hoechst33342 (Sigma–Aldrich) for 30 min at 37 °C. Then inserts were observed using an Inverted Microscope (Leica DM IRB) and acquired with Leica Qfluoro software. Quantification of invading cells was performed by counting Hoechst33342-stained nuclei in five random fields. Analysis was performed with ImageJ software. A minimum of three inserts was used for each sample to assess invasion. Invasion assay was performed on BCPAP cells silenced with MU-A, Timp-1 and siControl siRNAs for 48 h, and treated with rTIMP-1 and Akt inhibitor as described above.

Effects of TIMP-1 addition on BCPAP cell doxorubicin chemoresistance

BCPAP cells were plated in a 96-well plate in 100 µl serum-free medium/well. Cells were treated with: 100 or 250 ng/ml rTIMP-1; 100 nM TIMP-1 siRNA; 100 nM BRAF siRNA; TIMP-1 and BRAF siRNA combined; 10 µM Akt inhibitor. Cells were cultured with 2 µM doxorubicin up to 48 h. Cell proliferation was assessed by colorimetric assay using 3-(4,5-dimethylthiazol-2-yl)-2,5-diphenyltetrazolium bromide (MTT). Absorbance was read at 550 nm in a Multiskan FC microplate reader (Thermo Fisher Scientific). Apoptosis was evaluated by caspase-3 assay. Briefly, cells were fixed and permeabilized with Cytofix–Cytoperm kit (BD Pharmingen, Milan, Italy) according to the manufacturer's instructions. Data were analyzed with CELLQuest Pro software (Becton Dickinson). Gating was implemented based on negative control staining profiles.

Statistical analysis

Continuous variables are represented as mean ± S.D. Rates and proportions were calculated for dichotomic data and differences were analyzed by χ^2 test and Fisher exact test when appropriate. For continuous variables, nonparametric tests were used, and differences were analyzed by Mann–Whitney *U* test. Differences between paired continuous variables (mRNA expression of TIMP-1, in tumoral nodule vs contralateral healthy tissue) were analyzed by Wilcoxon test. $P<0.05$ was considered statistically significant. All analyses were performed with Statistical Package for Social Science (SPSS for Windows, v. 11.0, SPSS Italia, Bologna, Italy).

Results

NF-κB and MMP-9 are hyperactivated in BRAF^{V600E} PTC nodules compared with BRAF^{WT} nodules and their healthy contralateral lobes

NF-κB signaling pathway has been described as being upregulated in BRAF^{V600E} tumors (Ikenoue *et al.* 2004, Palona *et al.* 2006), including PTCs (71%; Mitsiades *et al.* 2006). The mutation has been associated with more aggressive histology/behavior. Concerning the underlying mechanism, BRAF^{V600E} apparently promotes activation of NF-κB independently of downstream MAPK signaling (Palona *et al.* 2006, Liu & Xing 2008). However, no precise correlation has been found between increased NF-κB activation and degree of malignant phenotype. Hence, we investigated NF-κB activation in BRAF^{V600E} mutated and BRAF^{WT} PTCs by electrophoretic mobility shift assay (EMSA; Kitchener *et al.* 2004). We found that NF-κB binding activity is increased in BRAF^{V600E} nodules in comparison to both BRAF^{WT} nodules and healthy counterparts (Fig. 1A). Thus, our findings confirmed that the NF-κB system is an important pathway involved in BRAF^{V600E} PTCs.

Tumor invasion is mediated by the action of MMPs, which are expressed more in tumor thyroid cells (Baldini *et al.* 2004, Yeh *et al.* 2006, Frasca *et al.* 2008). Metastasis formation is more common in BRAF^{V600E} PTCs (Xing 2007). Indeed, MMP overexpression has been induced upon expression of BRAF^{V600E} in several thyroid cell lines (Melillo *et al.* 2005, Mesa *et al.* 2006, Palona *et al.* 2006). We investigated the expression of MMPs in our PTCs by zymography. We observed higher proteolytic activity of MMP-9 in BRAF^{V600E} nodules in comparison to both BRAF^{WT} nodules and their healthy counterparts (Fig. 1B). Therefore, our findings support the role of the MMP system in mediating *BRAF^{V600E}* mutation-promoted progression of PTC.

TIMP-1 and its receptor CD63 are upregulated in BRAF^{V600E} PTC nodules compared with BRAF^{WT} nodules and their healthy contralateral lobes

TIMP-1 has been proposed as a good candidate gene involved in thyroid carcinogenesis in PTC (Griffith *et al.* 2006). We investigated TIMP-1 expression in BRAF^{V600E} and BRAF^{WT} PTC nodules and their respective healthy contralateral lobes. Microarray performed on 12 PTCs showed that BRAF^{V600E} PTC nodules are characterized by *TIMP-1* upregulation (4.03 ± 0.46-fold increase) in comparison to BRAF^{WT} nodules (0.98 ± 0.5-fold increase; $P<0.001$; Supplementary Figure 1A and B, see section on supplementary data given at the end of this article). Results were then validated by qRT-PCR in all 56 thyroid samples. PCR also showed that TIMP-1 was significantly upregulated in BRAF^{V600E} nodules compared with their healthy contralateral lobes ($P<0.001$). By contrast, no difference was found between BRAF^{WT} nodules and the healthy tissue ($P=0.405$; Fig. 1C).

It is well known that *TIMP-1* is negatively regulated by TWIST1 (Okamura *et al.* 2009). When we investigated *TWIST1* expression, as expected we found it downregulated in BRAF^{V600E} nodules in comparison to healthy contralateral lobes ($P=0.0014$). No difference was found between

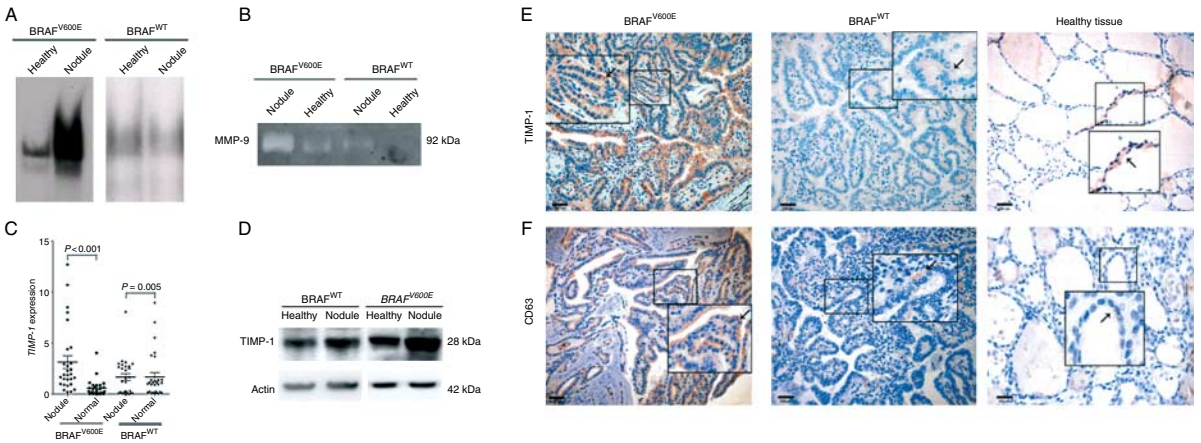

Figure 1 NF-κB, MMP-9, TIMP-1, and CD63 expression in BRAF^{V600E} and BRAF^{WT} PTCs. (A) EMSA analysis shows that NF-κB binding activity is increased in BRAF^{V600E} nodules (no. 16) in comparison to both BRAF^{WT} nodules (no. 16) and the respective contralateral healthy lobes (no. 16). Figure is representative of four independent experiments. (B) Zymography shows higher proteolytic activity of MMP-9 in BRAF^{V600E} nodules (no. 16) in comparison to both BRAF^{WT} nodules (no. 16) and the respective contralateral healthy lobes (no. 16). Figure is representative of five experiments. (C) qRT-PCR performed on 28 BRAF^{V600E} and 28 BRAF^{WT} PTCs shows that *TIMP-1* is upregulated in BRAF^{V600E} nodules in comparison to their respective contralateral healthy lobes ($P<0.001$), while no difference is found between BRAF^{WT} PTC nodules and healthy tissue ($P=0.405$). Differences were analyzed by Wilcoxon test. (D) Western blot analysis confirms TIMP-1 hyper-expression in PTCs harboring *BRAF^{V600E}* mutation (no. 16) in comparison to BRAF^{WT} PTCs (no. 16). The figure is representative of four experiments (see text for quantification). (E) TIMP-1 (cytoplasmic) is strongly expressed in BRAF^{V600E} PTC (left), weakly positive in BRAF^{WT} PTC (central), and very weakly positive in matched healthy tissue (right). (F) TIMP-1 receptor CD63 (cell membrane) is hyper-expressed in BRAF^{V600E} PTC (left) in comparison to both BRAF^{WT} PTC (central), and matched healthy tissue (right). Scale bar 100 μm. Inset shows higher magnification (40×). Arrows indicate positive cells.

BRAF^{WT} nodules and healthy tissues ($P=0.99$; Supplementary Figure 1C, see section on supplementary data given at the end of this article).

TIMP-1 expression was further confirmed by western blot analysis (densitometric analysis expressed as optical density units (OD): BRAF^{V600E} nodule 122.7 ± 6.7 vs BRAF^{WT} nodule 40.9 ± 25.9; $P=0.003$; Fig. 1D) and immunohistochemistry (TIMP-1 LI: BRAF^{V600E} nodule $71.48\pm15.67\%$ vs both BRAF^{WT} nodule $22.9\pm10.27\%$ and contralateral matched healthy tissue 12.7 ± 6.4; $P<0.001$; Fig. 1E).

CD63, a member of the tetraspanin family, has been indicated as TIMP-1 receptor in MCF10A human mammary epithelial cells (Jung *et al*. 2006). CD63 acts as a regulator of PI3K, FAK, Src, and Akt signaling pathways, which are implicated in the anti-apoptotic activity of TIMP-1 (Berditchevski & Odintsova 1999). Immunohistochemistry analysis confirmed higher expression of CD63 in BRAF^{V600E} in comparison to BRAF^{WT} nodules (CD63 LI: BRAF^{V600E} nodule $57.16\pm11.41\%$ vs BRAF^{WT} nodule $13.32\pm8.74\%$; $P<0.001$; Fig. 1F); contralateral matched healthy tissue resulted negative for CD63.

Proof of the principle

We hypothesized that a relationship exists between BRAF^{V600E}, NF-κB activation, and TIMP-1 hyper-expression. To validate this hypothesis we used well-established thyroid cell lines harboring or not *BRAF^{V600E}* mutation (Schweppe *et al*. 2008). We found that *TIMP-1* mRNA expression was significantly higher in BCPAP cell line (BRAF$^{V600E/V600E}$) in comparison to KTC-1 (BRAF$^{V600E/WT}$), TPC-1 (BRAF$^{WT/WT}$) cell lines, and normal thyroid mRNA (Fig. 2A). Flow cytometry analysis confirmed that BCPAP cells co-express TIMP-1 and CD63 ($75.6\pm3.2\%$; Fig. 2B). Thus, BCPAP cell line was considered a suitable and reproducible *in vitro* system for testing our hypothesis.

First, we aimed to verify whether BRAF^{V600E} activates NF-κB independently via MEK pathway, as previously suggested (Palona *et al*. 2006). Because BRAF is an upstream activator of MAPK kinase (MEK)/ERK pathway, we assessed the activation of MAPK pathway in BCPAP cell line by treating cells with U0126, a specific MEK inhibitor, and sorafenib, a multikinase inhibitor that targets several serine/threonine and receptor tyrosine kinases interacting with multiple intracellular (CRAF, BRAF, and mutant BRAF) and cell surface (KIT, FLT-3, VEGFR-2, VEGFR-3, and PDGFR-ß) kinases (Xing 2007). Treatment with both sorafenib and U0126 induced significant reduction of p-MEK assessed by WB (OD: sorafenib-treated BCPAP: 3.66 ± 1.52; U0126-treated BCPAP: 28.16 ± 2.02 vs untreated: 78.17 ± 2.02; $P<0.001$). In our experiments, only sorafenib was

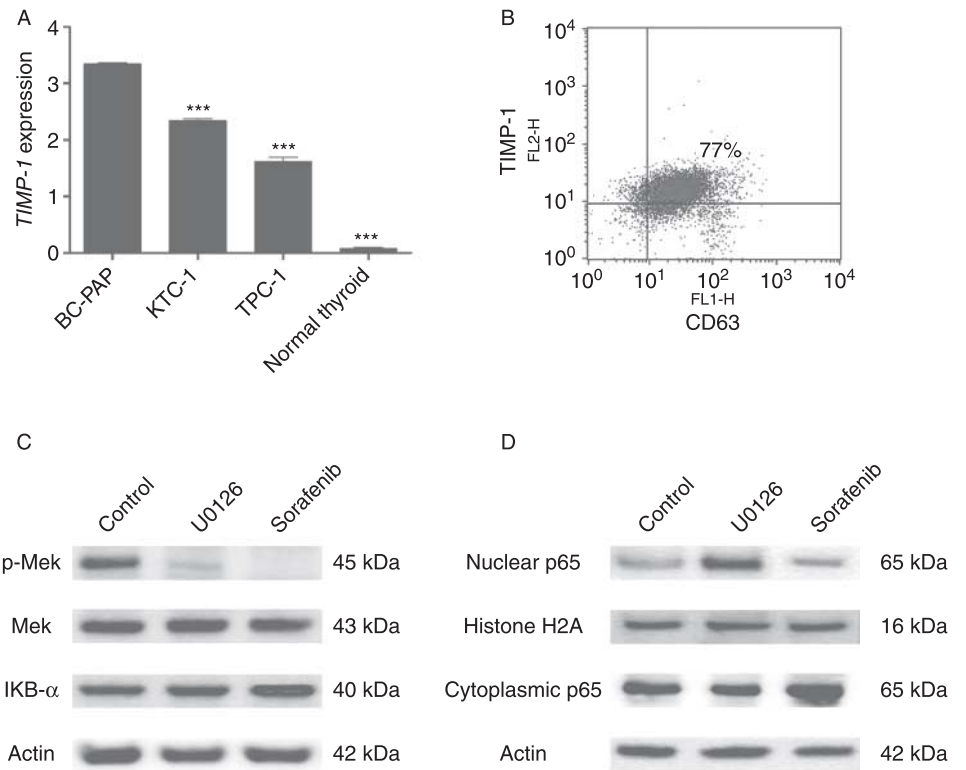

Figure 2 *TIMP-1* expression in thyroid cancer cell lines and normal thyroid tissue. (A) qRT-PCR shows that *TIMP-1* is expressed more in BCPAP (BRAF$^{V600E/V600E}$) and KTC-1 (BRAF$^{V600E/WT}$) in comparison to TPC-1 cell line (BRAF$^{WT/WT}$) and normal thyroid (BCPAP vs KTC-1, TPC-1, and normal thyroid; ***$P<0.001$). (B) Flow cytometry analysis confirms TIMP-1 and CD63 co-expression in BCPAP cells (mean±S.D.: 75.6±3.2%). BRAF^{V600E} is a strong activator of NF-κB, and this activating pathway is MEK-independent in BCPAP cells. BCPAP cells were treated with MAPK inhibitors U0126 (a specific MEK inhibitor), and sorafenib (a multikinase inhibitor that targets several serine/threonine and receptor tyrosine kinases). (C) Western blot analysis of total cell lysates from BCPAP cells treated for 4 h with 3 μM U0126 and 5 μM sorafenib. Both sorafenib and U0126 induced a significant reduction of p-MEK. However, only sorafenib treatment was able to increase the expression of IκB-α, an NF-κB specific inhibitor (OD: sorafenib-treated BCPAP vs untreated cells: 92.44±2.64 vs 69.2±2.15; $P=0.013$; U0126-treated BCPAP vs untreated cells: 65.5±2.1 vs 69.2±2.15; P=NS). (D) Western blot analysis of p65 subunit in nuclear and cytosolic proteins. Sorafenib treatment induced a specific hyper-expression of cytoplasmatic p65 (OD: treated cells vs untreated cells: 97.12±2.2 vs 65.7±3.1; $P=0.007$) while the nuclear fraction remained unchanged in comparison to untreated BCPAP (26.33±3.2 vs 24.56±3.5; P=NS). By contrast, U0126 determined high nuclear p65 hyper-expression (treated cells vs untreated cells: 90.2±3.2 vs 24.56±3.5; $P<0.001$) with concomitant cytoplasmatic reduction (treated cells vs untreated cells: 51.1±3.5 vs 65.7±3.1; P=NS). Anti-histone H2A and anti-β-actin were used as loading control. p, phosphorylated.

able to increase IκB-α expression (OD: sorafenib-treated BCPAP vs untreated cells: 92.44±2.64 vs 69.2±2.15, $P=0.013$; U0126-treated BCPAP vs untreated cells: 65.5±2.1 vs 69.2±2.15; P=NS; Fig. 2C). These results indicate that, in BCPAP cells, BRAF^{V600E} activates NF-κB and this pathway is MEK-independent.

As NF-κB is kept inactive in the cytoplasm by association with its specific inhibitor IκB-α, we evaluated the presence of the NF-κB subunit p65 in both cytoplasm and nucleus after treatment with both sorafenib and U0126. We found that sorafenib induced selective hyper-expression of p65 in the cytoplasm (OD: sorafenib-treated cells vs untreated cells: 97.12±2.2 vs 65.7±3.1; $P=0.007$), while the nuclear fraction remained unchanged (26.33±3.2 vs 24.56 ±3.5; P=NS). By contrast, U0126 determined nuclear p65 hyper-expression (treated cells vs untreated cells: 90.2±3.2 vs 24.56±3.5; $P<0.001$) with no significant concomitant cytoplasmatic reduction (treated cells vs untreated cells: 51.1±3.5 vs 65.7±3.1; P=NS; Fig. 2D).

To further verify the relationship between BRAF^{V600E}, NF-κB activation, and *TIMP-1* hyper-expression, we silenced the *BRAF* gene in BCPAP cell line using a specific siRNA for BRAF^{V600E} (MU-A). MU-A is incorporated into the RNA-induced silencing complex, promoting target mRNA degradation and/or translation. Silencing efficacy is shown in Fig. 3A and B. EMSA for NF-κB activation showed marked

reduction in NF-κB binding activity at 72 h post-silencing, thus confirming that NF-κB is regulated by $BRAF^{V600E}$ (Fig. 3C). At the same time points, qRT-PCR showed significantly decreased *TIMP-1* expression in MU-A-treated cells ($P=0.028$; Fig. 3D). As expected, $BRAF^{V600E}$ silencing in BCPAP cells also determined significant reduction in p-MEK protein expression with respect to untreated cells (OD: 26.23 $\pm$3.02 vs 45.21$\pm$4.7; $P=0.017$; Fig. 3E), demonstrating the efficiency of silencing. MU-A caused also reduction of Akt phosphorylation (OD: 32.5$\pm$2.5 vs 62.8$\pm$2.2; $P<0.001$), suggesting its involvement in

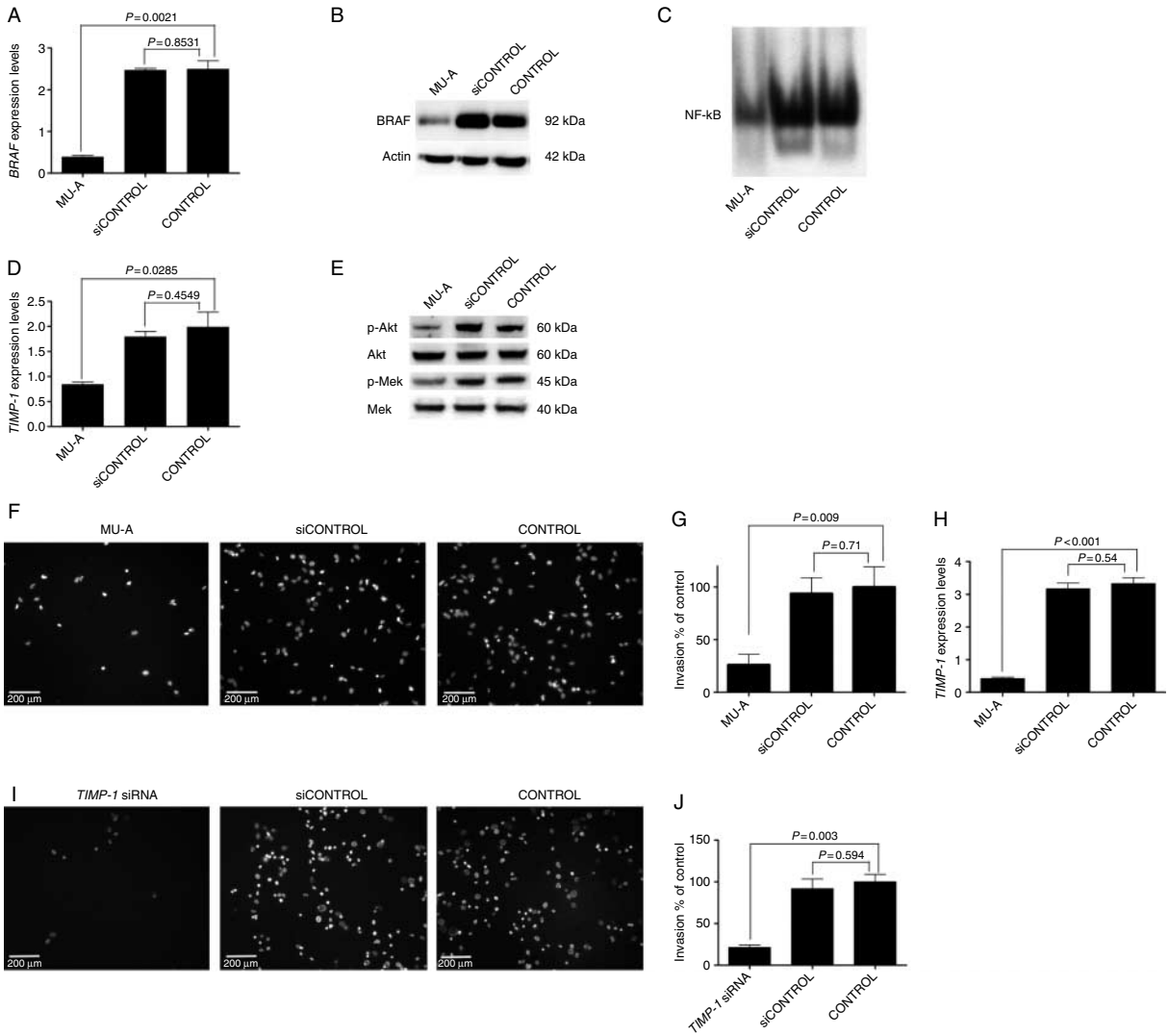

Figure 3 $BRAF^{V600E}$ regulates NF-κB activity, *TIMP-1* expression, and tumor invasion in BCPAP cell line. Silencing with a chemically synthesized siRNA targeting $BRAF^{V600E}$ mutation (MU-A) decreases BRAF mRNA and protein expression, resulting in reduction of NF-κB binding activity, *TIMP-1* expression, and cell invasion. (A) qRT-PCR shows that MU-A reduces *BRAF* expression in comparison to untreated cells ($P=0.002$). Data are normalized against *β-actin* gene expression. (B) Western blot analysis shows that MU-A decreases BRAF expression in comparison to scrambled siRNA (siCONTROL) and untreated cells. (C) EMSA shows that MU-A decreases NF-κB binding activity in comparison to both siCONTROL and untreated cells. (D) qRT-PCR shows that MU-A reduces *TIMP-1* expression in comparison to siCONTROL and untreated cells ($P=0.028$). (A and D) Data are representative of at least three independent experiments. (E) Western blot analysis of p-MEK, MEK, p-Akt, and Akt after silencing of BRAF with MU-A siRNA. (F) Invasiveness of BCPAP cells is reduced after $BRAF^{V600E}$ silencing with MU-A (left panel) in comparison to siCONTROL (central panel), and untreated cells (right panel). Scale bar 200 μm. (G) Quantification of cell invasiveness. Percentages of cell migration after $BRAF^{V600E}$ silencing considering control as equal to 100%. (H) qRT-PCR shows that TIMP-1 siRNA reduces *TIMP-1* expression in comparison to untreated cells ($P<0.001$). Data are normalized against *β-actin* gene expression. (I) Invasiveness of BCPAP cells is reduced after *TIMP-1* silencing (left panel) in comparison to siCONTROL (central panel), and untreated cells (right panel). Scale bar 200 μm. (J) Quantification of cell invasiveness. Percentages of cell migration after *TIMP-1* silencing considering control as equal to 100%. Data are representative of three independent experiments. Bars indicate mean$\pm$S.D. of the data collected in triplicate.

the regulation of cell proliferation. Furthermore, we evaluated whether BRAF^{V600E} inhibition can affect invasion in BCPAP cells after treatment with MU-A. After 24 h in a BioCoated Matrigel chamber, MU-A-treated cells significantly decreased their ability to invade ($P=0.009$; Fig. 3F and G), thus proving *BRAF^{V600E}* mutation also exerts a pivotal role in regulating tumor invasion. The same decrease in invasion ability was found after TIMP-1 silencing ($P=0.003$; Fig. 3H, I, and L).

To investigate the relationship between NF-κB and TIMP-1, we treated BCPAP cells with dexamethasone, a generic inhibitor of the inflammatory pathway; parthenolide, a specific NF-κB inhibitor; and MG-132, a proteasome inhibitor blocking IκB-α degradation (Revest *et al*. 2005, Domingo-Domènech *et al*. 2008, Zhang *et al*. 2009). We then evaluated *TIMP-1* expression by qRT-PCR. Our results showed remarkable downregulation of *TIMP-1* (Fig. 4A) which was confirmed by flow cytometry and IF. In particular, TIMP-1 expression was consistently reduced after parthenolide (Fig. 4B–E, Supplementary Figure 2, see section on supplementary data given at the end of this article). By contrast, *TIMP-1* silencing did not affect either *BRAF^{V600E}* expression or NF-κB activity (Supplementary Figure 3A and B, see section on supplementary data given at the end of this article).

BRAF^{V600E}/NF-κB/TIMP-1/CD63 pathway exists in BCPAP cell line

It has been demonstrated in colorectal and breast cancer that TIMP-1 binding with CD63 upregulates cell proliferation through Akt phosphorylation at Ser-473 (Stetler-Stevenson 2008). To clarify whether TIMP-1 activates Akt phosphorylation in PTC, we forced expression of TIMP-1 in BCPAP cell line by treatment with recombinant TIMP-1 at different concentrations (10–250 ng/ml) and time points (30 and 60 min). BrdU proliferation assay showed that cells treated with rTIMP-1 exhibit concentration-dependent proliferative activity compared with untreated cells, with higher values at 250 ng/ml (Fig. 5A). Indeed, treatment with 250 ng/ml rTIMP-1 already induced Akt phosphorylation at 30 min in comparison to untreated cells (OD: $30'=25.11\pm1.01$ and $60'=20.22\pm1.34$ vs 6.45 ± 0.74; $P=0.002$ and $P=0.004$ respectively; Fig. 5B).

We then investigated the Akt-dependent proliferative activity of TIMP-1. To this end, we treated BCPAP cells with doxorubicin after addition of exogenous rTIMP-1, 10 μM Akt inhibitor and silencing of *TIMP-1* and/or *BRAF*. As expected, cell viability was significantly increased in rTIMP-1-treated cells in a dose-dependent manner. By contrast, it was reduced after

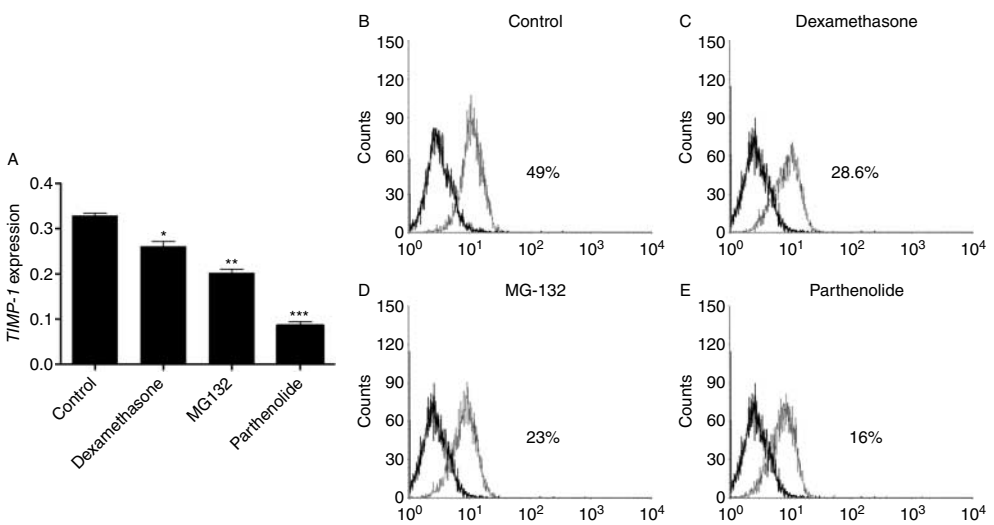

Figure 4 *TIMP-1* expression is significantly reduced after treatment with NF-κB inhibitors. BCPAP cells were stimulated for 24 h with 5 μM MG-132 (proteasome inhibitor), 50 nM dexamethasone 21-phosphate (non-specific NF-κB inhibitor), and 10 μM parthenolide (specific NF-κB inhibitor) in the presence of monensin, and evaluated by qRT-PCR and flow cytometry. (A) qRT-PCR shows a major reduction in *TIMP-1* expression after treatment with all three drugs. This reduction is higher with parthenolide, which is a specific NF-κB inhibitor. *$P=0.014$; **$P=0.003$; and ***$P<0.001$. (B–E) Quantification of TIMP-1 expression by flow cytometry confirms higher decrease after parthenolide (E), in comparison to MG-132 (D), dexamethasone (C) treated cells, and control cells (B). Cells were incubated for 30 min with PE-labeled TIMP-1 monoclonal antibody (gray lines). Solid black lines represent control cells stained with PE-secondary isotype-matched antibody. Percentages of TIMP-1-positive cells are indicated as a representative experiment. About 2×10^4 cells per experimental condition of three independent experiments were analyzed in duplicates.

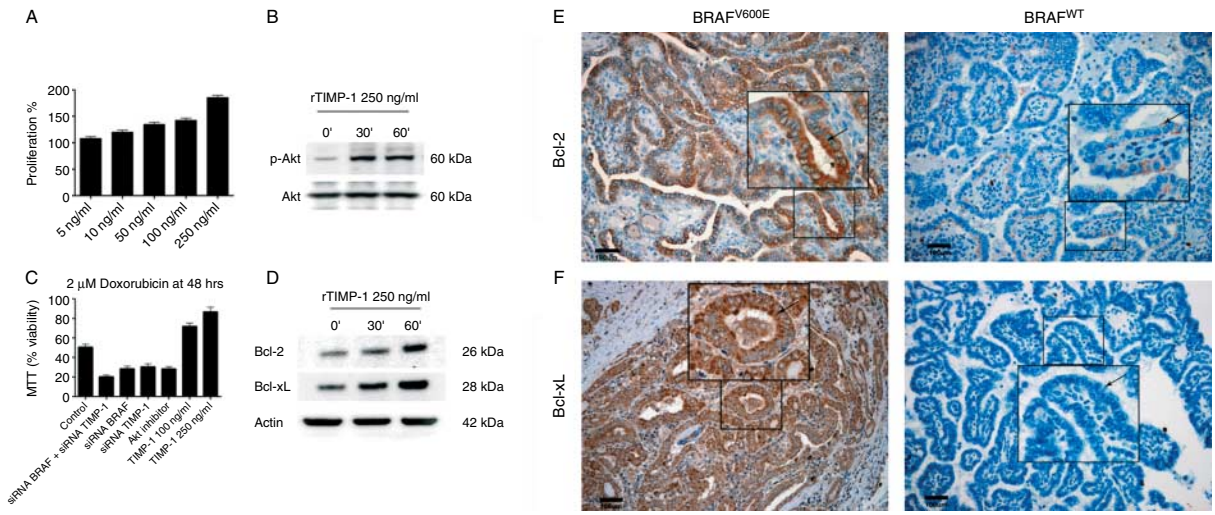

Figure 5 Treatment of BCPAP cell line with rTIMP-1 increases cell proliferation, induces Akt phosphorylation, determines doxorubicin resistance. (A) BCPAP cells were incubated for 24 h with rTIMP-1 at different concentrations. The amount of newly synthesized DNA in proliferating cells measured by BrdU incorporation assay increased directly to rTIMP-1 concentrations. (B) Cells were treated with rTIMP-1 (250 ng/ml) for 30 and 60 min. Western blot analysis was performed with Akt and p-Akt specific antibodies. Treatment already induced Akt phosphorylation after 30 min in comparison to untreated cells. (C) BCPAP cell line was cultured for 48 h with 2 μM doxorubicin in the presence of 100 or 250 ng/ml rTIMP-1; 10 μM Akt inhibitor VIII; 100 nM TIMP-1 siRNA; 100 nM BRAF siRNA; TIMP-1 and BRAF siRNA combined. Results showed reduced cell viability (MTT) after TIMP-1 siRNA, BRAF siRNA, and TIMP-1 + BRAF siRNA and Akt inhibitor whereas it increased after rTIMP-1 addition. (D) Hyper-expression of Bcl-xL and Bcl-2 in BCPAP cells treated with 250 ng/ml rTIMP-1. Data are representative of three independent experiments. (E) Bcl-2 is strongly expressed in $BRAF^{V600E}$ PTC (left) and weakly positive in $BRAF^{WT}$ PTC (right). (F) Bcl-xL is hyper-expressed in $BRAF^{V600E}$ PTC (left) in comparison to $BRAF^{WT}$ PTC (right). Scale bar 100 μm. Insets show higher magnification (40×).

silencing with single or combined BRAF and TIMP-1 siRNA and after treatment with Akt inhibitor (Fig. 5C). The decreased viability was not related to caspase-3 (data not shown). These data collectively confirm the faculty of TIMP-1 to confer resistance to doxorubicin-treated BCPAP cells. To further assess targets of Akt that are involved in regulation of cell proliferation and apoptosis, we also evaluated Bcl-2 and Bcl-xL expression in cells treated with 250 ng/ml recombinant TIMP-1. We found that the expression of both anti-apoptotic molecules increased significantly in comparison to untreated cells ((Bcl-2 OD: $30' = 26.3 \pm 1.5$ and $60' = 46 \pm 1$ vs 17 ± 2.6; $P = 0.023$ and $P = 0.001$, respectively); (Bcl-xL OD: $30' = 65.66 \pm 3.5$ and $60' = 76.6 \pm 2.08$ vs 36.3 ± 1.5; $P = 0.004$ and $P < 0.001$ respectively); Fig. 5D). As expected, both Bcl-2 and Bcl-xL proved to be hyper-expressed (Fig. 5E and F) in $BRAF^{V600E}$ in comparison to $BRAF^{WT}$ PTCs (Bcl-2 LI: $BRAF^{V600E}$ nodule $69.38 \pm 14.72\%$ vs $BRAF^{WT}$ nodule $11.84 \pm 3.62\%$; $P < 0.001$. Bcl-xL LI: $BRAF^{V600E}$ nodule $83.21 \pm 17.46\%$ vs $BRAF^{WT}$ nodule $13.25 \pm 4.18\%$; $P < 0.001$).

To further evaluate the role of TIMP-1 and Akt expression in tumor invasiveness we performed an invasion assay after treatment with rTIMP-1 or Akt inhibitors. We found that rTIMP-1 stimulated cell invasion ($P = 0.003$), while after Akt inhibition a significant reduction in cell invasion (>50%) was observed (***$P < 0.001$; Fig. 6A and B). These results demonstrated that the role of TIMP-1 in cell invasion and proliferation is mediated by Akt phosphorylation. Indeed, when we considered BCPAP cell proliferation after specific Akt inhibition we found a significant decrease in cell proliferation in comparison to untreated cells (70–85%; $P = 0.010$; Fig. 6C). Since MEK inhibitors are currently used in clinical trials for the treatment of thyroid cancers, we further explored whether Akt phosphorylation was influenced by sorafenib and U0126 treatment by western blot. As expected, p-Akt protein expression in BCPAP was significantly reduced after sorafenib in comparison to untreated cells (OD: 33.15 ± 2.01 vs 45.25 ± 2.04, $P < 0.001$), but no difference was found after UO126 treatment (OD: 47 ± 1 vs 45.25 ± 2.04, $P =$ NS; Fig. 6D). As shown in Fig. 6E, *TIMP-1* mRNA expression in BCPAP proved to be strongly decreased, by more than 50%, after sorafenib treatment in comparison to the reduction observed in U0126-treated BCPAP cells (above 20%).

Figure 7 summarizes the proposed molecular mechanism for the interaction of $BRAF^{V600E}$, NF-κB, and TIMP-1.

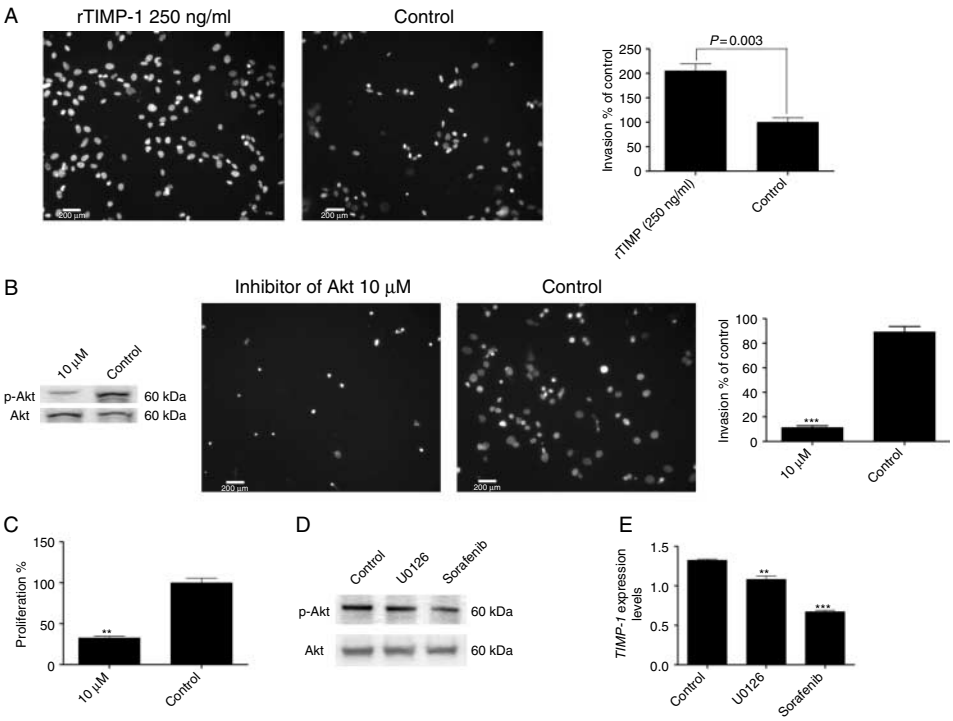

Figure 6 BCPAP cell invasiveness after addition of rTIMP-1 and Akt inhibition. (A) Invasiveness of BCPAP cells increases after treatment with rTIMP-1 (left panel) in comparison to untreated cells (right panel). Scale bar 200 μm. Graph shows quantification of cell invasion (percentage indicates cell migration after rTIMP-1 treatment considering control as equal to 100%). Data are represented as mean±S.D. of three independent experiments. (B) 10 μM Akt inhibitor causes reduction of Akt phosphorylation (left panel) and decreased cell invasiveness in comparison to untreated cells (center panel). Scale bar 200 μm. Graph (right panel) shows quantification of cell invasion. Percentages of cell migration after Akt inhibitor treatment considering control as equal to 100%. Data are represented as mean±S.D. of three independent experiments. (C) Reduction of BCPAP cell proliferation after Akt inhibition in treated in comparison to untreated cells evaluated by BrDU assay (**$P=0.010$). (D) Reduction of p-Akt protein expression in BCPAP after sorafenib in comparison to untreated cells ($P<0.001$); no difference was found after treatment with UO126. (E) TIMP-1 mRNA expression was more significantly reduced after sorafenib than after U0126 treatment in comparison to untreated cells. Data are represented as mean±S.D. of three independent experiments. **$P=0.024$ and ***$P<0.001$.

Discussion

BRAF, a serine/threonine kinase known to activate the MAPK pathway, has been found mutated in several tumors, namely melanoma, colorectal carcinoma, and thyroid carcinoma (Karasarides *et al*. 2004, Liu *et al*. 2007, Preto *et al*. 2008). In thyroid carcinomas the molecules and pathways associated with the effect of BRAF inhibition in cellular proliferation and survival are not fully understood. Our study demonstrates the existence of a trilogy involving BRAF^{V600E}, NF-κB, and TIMP-1 in *ex vivo* PTCs. We provided proof of the principle by using an *in vitro* model that confirmed that BRAF^{V600E} activates NF-κB and subsequently increases TIMP-1 expression, which in turn binds CD63 leading to Akt phosphorylation. This pathway eventually results in increased proliferation and invasiveness, inhibition of apoptosis and resistance to doxorubicin.

We found that BRAF^{V600E}-mutated PTC nodules hyper-express TIMP-1. TIMP-1 is known to be a specific inhibitor of MMP-9. Conditional expression of BRAF was associated with markedly increased invasion of Matrigel compared with cells expressing RET/PTC3 (Mesa *et al*. 2006); this mechanisms may be involved in extrathyroidal invasion and metastasis of PTCs harboring BRAF^{V600E}. In this study, we confirm increased MMP-9 expression and activity in PTC nodules, along with TIMP-1 hyper-expression. The role played by BRAF^{V600E} in cell invasion was proved on BCPAP cells after silencing along with remarkable inhibition of cell invasiveness.

We also found hyperactivation of the NF-κB system, which we propose could be the link between *BRAF^{V600E}* mutation and TIMP-1 hyper-expression. Silencing of BRAF^{V600E} resulted in decreased NF-κB and TIMP-1 expression. This observation suggests that *BRAF^{V600E}* mutation is an upstream event. CRAF, which is another isoform of RAF family proteins, has been shown to activate NF-κB in NIH3T3 cells (Vale *et al*. 2001). On the other hand, NF-κB is

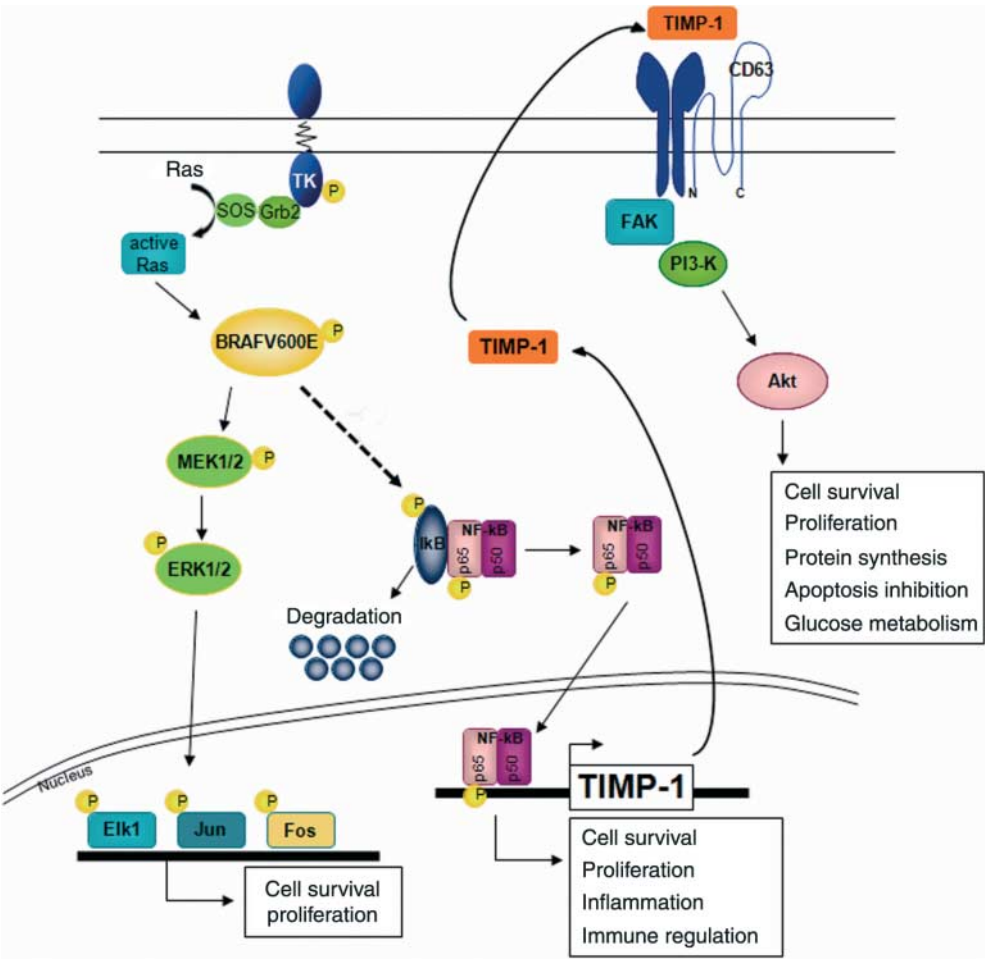

Figure 7 Proposed molecular mechanism for the interaction of BRAF^{V600E}, NF-κB, and TIMP-1. Left: BRAF conventional pathway. Right: proposed BRAF^{V600E} pathway. BRAF^{V600E} induces p-IκBα and subsequent degradation→NF-κB activation→increased TIMP-1 expression→TIMP-1 binds CD63→Akt is phosphorylated→activation of anti-apoptosis and proliferation.

advocated as playing an important role in a variety of thyroid cancers. In the present work, silencing of BRAF with MAPK inhibitors clearly acts on IκB-α, a cytoplasmatic inhibitor of NF-κB, controlling the translocation of p65 into the nucleus (Karin 2006). In our study, we confirm that NF-κB activation is independent of MEK pathway. Furthermore, our findings suggest that the mutation in our series of BRAF^{V600E} PTCs could influence NF-κB activation through IκB-α phosphorylation. Activated NF-κB translocates into the nucleus inducing the transcription of several known genes (Baud & Karin 2009). In fact, in our study NF-κB activation results in increased TIMP-1 expression.

Increased NF-κB activity is associated with thyroid carcinogenesis and tumor progression. In particular, it has been reported that activation of MAPK pathway by BRAF^{V600E} is involved in the pathogenesis of PTC (Fusco *et al*. 1987, Kimura *et al*. 2003). Conversely, MAPK has also been showed to induce activation of NF-κB signaling (Tuyt *et al*. 1999). Degradation of IκB-α takes place shortly after ectopic accumulation of the BRAF^{V600E} protein, resulting in the activation of NF-κB signaling via MEK–ERK-independent pathway (Palona *et al*. 2006). In line with these observations, a previous study demonstrated that oncogenic Ret-induced NF-κB activity depends on IKK-mediated IκB-α degradation and requires functional Ras, Raf, and MEKK1 and that NF-κB activation is not accomplished by MEK/ERK activation (Ludwig *et al*. 2001).

Silencing of TIMP-1 did not affect either BRAF^{V600E} or NF-κB, confirming that TIMP-1 is the downstream factor of the trilogy. The link between these two players is NF-κB, as demonstrated by the decrease in TIMP-1 expression when NF-κB inhibitors were used.

We also identified one of the possible MMP-9-independent molecular mechanisms by which TIMP-1 exerts its biological activity on cell proliferation. TIMP-1 binds its receptor CD63 on cell membrane and activates Akt signaling pathway responsible for its anti-apoptotic activity (Stetler-Stevenson 2008). Akt exerts its effects in the cell by phosphorylating a variety of downstream substrates, all resulting in anti-apoptotic, or pro-proliferative effects (Shinohara *et al*. 2007). CD63 was found to be expressed in PTC specimens and in BCPAP cells. Addition of recombinant TIMP-1 protein in our *in vitro* model resulted in enhanced Akt phosphorylation, eventually leading to increased proliferation. These results are consistent with the anti-apoptotic activity of TIMP-1 mediated by CD63-binding (Stetler-Stevenson 2008). In addition, TIMP-1 increases Bcl-xL and Bcl-2 expression via Akt, confirming the crucial involvement of the PI3K/AKT pathway in TIMP-1 signaling (Guedez *et al*. 1998). Interestingly, in human breast epithelial cells, overexpression of Bcl-2 also proved to be associated with increased levels of TIMP-1 (Li *et al*. 1999). Subsequent studies showed that TIMP-1 is a potent inhibitor of apoptosis induced by a variety of intrinsic apoptotic stimuli. In fact, TIMP-1 causes phosphorylation of FAK, which in turn activates PI3-kinase and subsequently Akt, resulting in Bcl-2 and Bcl-xL activation (Liu *et al*. 2005).

Currently, promising therapeutic approaches targeting BRAF are being tested in clinical trials, particularly in more aggressive PTC (Lassalle *et al*. 2010). In this perspective, our findings suggest that targeting the described trilogy might be a more effective strategy for aggressive forms of PTC.

Supplementary data

This is linked to the online version of the paper at http://dx.doi.org/10.1530/ERC-11-0076.

Declaration of interest

The authors declare that there is no conflict of interest that could be perceived as prejudicing the impartiality of the research reported.

Funding

This work was partially supported by the Italian Ministry of Health (C Giordano), the Sicilian Government Healthcare Department (C Giordano) and the University of Palermo, Italy (ex 60%, C Giordano). A Bommarito is recipient of MIUR research fellowship.

Author contribution statement

A Bommarito, P Richiusa, and E Carissimi conception and design, collection and assembly of data, data analysis and interpretation, manuscript writing; G Pizzolanti, V Rodolico, G Zito, A Criscimanna, F Di Blasi, M Pitrone, M Zerilli, M C Amato, G Spinelli, V Carina, G Modica, and M A Latteri collection and assembly of data, data analysis and interpretation; A Galluzzo conception and design financial support, final approval of manuscript; C Giordano conception and design, data analysis and interpretation, financial support, manuscript writing.

Acknowledgements

The authors thank Prof. S Feo for his help in microarray analysis; Prof. A Belfiore (University of Catanzaro, Italy) and Dr Riccardo Di Fiore (University of Palermo, Italy) for thoughtful suggestions; Drs D Forti, M Nucera, L Smeraldi, R Modica, and V Bullara for their efforts in the collection of thyroid samples; and Prof. Denis Gailor for revising the English. BCPAP cell line was kindly provided by Prof. F Frasca, University of Catania, Italy. KTC-1 cell line was kindly provided by Dr J Kurebayashi, Kawasaki Medical School, Japan.

References

Baldini E, Toller M, Graziano FM, Russo FP, Pepe M, Biordi L, Marchioni E, Curcio F, Ulisse S, Ambesi-Impiombato FS *et al.* 2004 Expression of matrix metalloproteinases and their specific inhibitors in normal and different human thyroid tumor cell lines. *Thyroid* **14** 881–888. (doi:10.1089/thy.2004.14.881)

Baud V & Karin M 2009 Is NF-kappaB a good target for cancer therapy? Hopes and pitfalls *Nature Reviews. Drug Discovery* **8** 33–40. (doi:10.1038/nrd2781)

Berditchevski F & Odintsova E 1999 Characterization of integrin–tetraspanin adhesion complexes: role of tetraspanins in integrin signaling. *Journal of Cell Biology* **146** 477–492. (doi:10.1083/jcb.146.2.477)

Cooper DS, Doherty GM, Haugen BR, Kloos RT, Lee SL, Mandel SJ, Mazzaferri EL, McIver B, Sherman SI & Tuttle RM 2006 Management guidelines for patients with thyroid nodules and differentiated thyroid cancer. *Thyroid* **16** 109–142. (doi:10.1089/thy.2006.16.109)

Davies L & Welch HG 2006 Increasing incidence of thyroid cancer in the United States 1973–2002. *Journal of the American Medical Association* **295** 2164–2167. (doi:10.1001/jama.295.18.2164)

Davies H, Bignell GR, Cox C, Stephens P, Edkins S, Clegg S, Teague J, Woffendin H, Garnett MJ & Bottomley W 2002 Mutations of BRAF gene in human cancer. *Nature* **417** 949–954. (doi:10.1038/nature00766)

Deryugina EI & Quigley IP 2006 Matrix metalloproteinases and tumor metastasis. *Cancer Metastasis Reviews* **25** 9–34. (doi:10.1007/s10555-006-7886-9)

Dhomen N & Marais R 2007 New insight into BRAF mutations in cancer. *Current Opinion in Genetics & Development* **17** 31–39. (doi:10.1016/j.gde.2006.12.005)

Domingo-Domènech J, Pippa R, Tápia M, Gascón P, Bachs O & Bosch M 2008 Inactivation of NF-kappaB by proteasome inhibition contributes to increased apoptosis induced by histone deacetylase inhibitors in human breast cancer cells. *Breast Cancer Research and Treatment* **112** 53–62. (doi:10.1007/s10549-007-9837-8)

Fontaine JF, Mirebeau-Prunier D, Raharijaona M, Franc B, Triau S, Rodien P, Goëau-Brissonniére O, Karayan-Tapon L, Mello M, Houlgatte R *et al.* 2009 Increasing the number of thyroid lesions classes in microarray analysis improves the relevance of diagnostic markers. *PLoS ONE* **4** e7632. (doi:10.1371/journal.pone.0007632)

Frasca F, Nucera C, Pellegriti G, Gangemi P, Attard M, Stella M, Loda M, Vella V, Giordano C, Trimarchi F *et al.* 2008 BRAF(V600E) mutation and the biology of papillary thyroid cancer. *Endocrine-Related Cancer* **15** 191–205. (doi:10.1677/ERC-07-0212)

Fusco A, Grieco M, Santoro M, Berlingieri MT, Pilotti S, Pierotti MA, Della Porta G & Vecchio G 1987 A new oncogene in human thyroid papillary carcinomas and their lymph-nodal metastases. *Nature* **328** 170–172. (doi:10.1038/328170a0)

Garnett MJ & Marais R 2004 Guilty as charged: B-RAF is a human oncogene. *Cancer Cell* **6** 313–319. (doi:10.1016/j.ccr.2004.09.022)

Griffith OL, Melck A, Jones SJM & Wiseman SM 2006 Meta-analysis and meta-review of thyroid cancer gene expression profiling studies identifies important diagnostic biomarkers. *Journal of Clinical Oncology* **24** 5043–5505. (doi:10.1200/JCO.2006.06.7330)

Guedez L, Stetler-Stevenson WG, Wolff L, Wang J, Fukushima P, Mansoor A & Stetler-Stevenson M 1998 *In vitro* suppression of programmed cell death of B cells by tissue inhibitor of metalloproteinases-1. *Journal of Clinical Investigation* **102** 2002–2010. (doi:10.1172/JCI2881)

Hawthorn L, Stein L, Varma R, Wiseman S, Loree T & Tan D 2004 TIMP1 and SERPIN-A overexpression and TFF3 and CRABP1 underexpression as biomarkers for papillary thyroid carcinoma. *Head & Neck* **26** 1069–1083. (doi:10.1002/hed.20099)

Hingorani SR, Jacobetz MA, Robertson GP, Herlyn M & Tubeson DA 2003 Suppression of BRAF(V599E) in human melanoma abrogates transformation. *Cancer Research* **63** 5198–5202.

Hsu ChY, Ming-Tak D, Yang Ch F & Chiang H 2003 Interobserver reproducibility of MIB-1 labeling index in astrocytic tumors using different counting methods. *Modern Pathology* **16** 951–957. (doi:10.1097/01.MP.0000084631.64279.BC)

Hundahl SA, Fleming ID, Fremgen AM & Menck HR 1998 A National Cancer Data Base report on 53,856 cases of thyroid carcinoma treated in U.S., 1985–1995. *Cancer* **83** 2638–2648. (doi:10.1002/(SICI)1097-0142(19981215)83:12<2638::AID-CNCR31>3.0.CO;2-1)

Ikenoue T, Hikiba Y, Kanai F, Aragaki J, Tanaka Y, Imamura J, Imamura T, Ohta M, Ijichi H, Tateishi K *et al.* 2004 Different effects of point mutations within the B-Raf glycine-rich loop in colorectal tumors on mitogen-activated protein/extracellular signal-regulated kinase kinase/extracellular signal-regulated kinase and nuclear factor B pathway and cellular transformation. *Cancer Research* **64** 3428–3435. (doi:10.1158/0008-5472.CAN-03-3591)

Jung KK, Liu XW, Chirco R, Fridman R & Kim HR 2006 Identification of CD63 as a tissue inhibitor of metalloproteinase-1 interacting cell surface protein. *EMBO Journal* **25** 3934–3942. (doi:10.1038/sj.emboj.7601281)

Karasarides M, Chiloeches A, Hayward R, Niculescu-Duvaz D, Scanlon I, Friedlos F, Ogilvie L, Hedley D, Martin J, Marshall CJ *et al.* 2004 B-RAF is a therapeutic target in melanoma. *Oncogene* **23** 6292–6298. (doi:10.1038/sj.onc.1207785)

Karin M 2006 Nuclear factor-kB in cancer development and progression. *Nature* **441** 431–436. (doi:10.1038/nature04870)

Kimura ET, Nikiforova MN, Zhu Z, Knauf JA, Nikiforov YE & Fagin JA 2003 High prevalence of BRAF mutations in thyroid cancer: genetic evidence for constitutive activation of the RET/PTC-RAS-BRAF signaling pathway in papillary thyroid carcinoma. *Cancer Research* **63** 1454–1457.

Kitchener P, Di Blasi F, Borrelli E & Piazza PV 2004 Differences between brain structures in nuclear translocation and DNA binding of the glucocorticoid receptor during stress and the circadian cycle. *European Journal of Neuroscience* **19** 1837–1846. (doi:10.1111/j.1460-9568.2004.03267.x)

La Rocca G, Pucci-Minafra I, Marrazzo A, Taormina P & Minafra S 2004 Zymographic detection and clinical correlation of MMP2 and MMP9 in breast cancer sera. *British Journal of Cancer* **90** 1414–1421. (doi:10.1038/sj.bjc.6601725)

Lassalle S, Hofman V, Ilie M, Butori C, Bozec A, Santini J, Vielh P & Hofman P 2010 Clinical impact of the detection of BRAF mutations in thyroid pathology: potential usefulness as diagnostic, prognostic and theragnostic applications. *Current Medicinal Chemistry* **17** 1839–1850. (doi:10.2174/092986710791111189)

Leenhardt L, Grosclaude P & Cherie-Challine L 2004 Increased incidence of thyroid carcinoma in France: a true epidemic or thyroid nodule management effects? Report from the French Thyroid Cancer Committee *Thyroid* **14** 1056–1060. (doi:10.1089/thy.2004.14.1056)

Li G, Fridman R & Kim HR 1999 Tissue inhibitor of metalloproteinase-1 inhibits apoptosis of human breast epithelial cells. *Cancer Research* **59** 6267–6275.

Liu D & Xing M 2008 Potent inhibition of thyroid cancer cells by the MEK inhibitor PD0325901 and its potentiation by suppression of the PI3K and NF-kB pathways. *Thyroid* **18** 853–864. (doi:10.1089/thy.2007.0357)

Liu XW, Taube ME, Jung KK, Dong Z, Lee YJ, Roshy S, Sloane BF, Fridman R & Kim HR 2005 Tissue inhibitor of metalloproteinase-1 protects human breast epithelial cells from extrinsic cell death: a potential oncogenic activity of tissue inhibitor of metalloproteinase-1. *Cancer Research* **65** 898–906.

Liu D, Liu Z, Condouris S & Xing M 2007 BRAFV600E maintains proliferation, transformation and tumorigenicity of BRAF-mutant papillary thyroid cancer cells. *Journal of Clinical Endocrinology and Metabolism* **92** 2264–2271. (doi:10.1210/jc.2006-1613)

Ludwig L, Kessler H, Wagner M, Hoang-Vu C, Dralle H, Adler G, Böhm BO & Schmid RM 2001 Nuclear factor-κB is constitutively active in C-cell carcinoma and required for RET-induced transformation. *Cancer Research* **61** 64–67.

Melillo RM, Castellone MD, Guarino V, De Falco V, Cirafici AM, Salvatore G, Caiazzo F, Basolo F, Giannini R, Kruhoffer M *et al.* 2005 The RET/PTC-RAS-BRAF linear signaling cascade mediates the motile and mitogenic phenotype of thyroid cancer cells. *Journal of Clinical Investigation* **115** 1068–1081. (doi:10.1172/JCI22758)

Mesa C, Mirza M, Mitsutake N, Sartor M, Medvedovic M, Tomlinson C, Knauf JA, Weber GF & Fagin JA 2006 Conditional activation of RET/PTC3 and BRAFv600E in thyroid cells is associated with gene expression profiles that predict a preferential role of BRAF in extra cellular matrix remodeling. *Cancer Research* **66** 6521–6529. (doi:10.1158/0008-5472.CAN-06-0739)

Mitsiades CS, Kotoula V, Poulaki V, Sozopoulos E, Negri J, Charalambous E, Fanourakis G, Voutsinas G, Tseleni-Balafouta S & Mitsiades N 2006 Epidermal growth factor receptor as a therapeutic target in human thyroid carcinoma: mutational and functional analysis. *Journal of Clinical Endocrinology and Metabolism* **91** 3662–3666. (doi:10.1210/jc.2006-0055)

Okamura H, Yoshida K & Haneji T 2009 Negative regulation of TIMP1 is mediated by transcription factor TWIST1. *International Journal of Oncology* **35** 181–186. (doi:10.3892/ijo_00000327)

Pacifico F & Leonardi A 2010 Role of NF-kappaB in thyroid cancer. *Molecular and Cellular Endocrinology* **321** 29–35. (doi:10.1016/j.mce.2009.10.010)

Palona I, Namba H, Mitsutake N, Starenki D, Podtcheko A, Sedliarou I, Ohtsuru A, Saenko V, Nagayama Y, Umezawa K *et al.* 2006 BRAFv600E promotes invasiveness of thyroid cancer cells through nuclear factor kB activation. *Endocrinology* **147** 5699–5707. (doi:10.1210/en.2006-0400)

Pizzolanti G, Russo L, Richiusa P, Bronte V, Nuara RB, Rodolico V, Amato MC, Smeraldi L, Sisto PS, Nucera M *et al.* 2007 Fine-needle aspiration molecular analysis for the diagnosis of papillary thyroid carcinoma through BRAF V600E mutation and RET/PTC rearrangement. *Thyroid* **17** 1109–1115. (doi:10.1089/thy.2007.0008)

Preto A, Figueiredo J, Velho S, Ribeiro AS, Soares P, Oliveira C & Seruca R 2008 BRAF provides proliferation and survival signals in MSI colorectal carcinoma cells displaying BRAF (V600E) but not KRAS mutations. *Journal of Pathology* **214** 320–327. (doi:10.1002/path.2295)

Revest JM, Di Blasi F, Kitchener P, Rougé-Pont F, Desmedt A, Turiault M, Tronche F & Piazza PV 2005 The MAPK pathway and Egr-1 mediate stress-related behavioral effects of glucocorticoids. *Nature Neuroscience* **8** 664–672 (Erratum in: *Nature Neuroscience* **8** 835). (doi:10.1038/nn1441)

Rodolico V, Cabibi D, Pizzolanti G, Richiusa P, Gebbia N, Martorana A, Russo A, Amato MC, Galluzzo A & Giordano C 2007 BRAF (V600E) mutation and p27(kip) expression in papillary carcinomas of the thyroid $\leq$1 cm and their paired lymph node metastases. *Cancer* **110** 1218–1226. (doi:10.1002/cncr.22912)

Schlumberger MJ 1998 Papillary and follicular thyroid carcinoma. *New England Journal of Medicine* **338** 297–306. (doi:10.1056/NEJM199801293380506)

Schweppe RE, Klopper JP, Korch C, Pugazhenthi U, Benezra M, Knauf JA, Fagin JA, Marlow LA, Copland JA, Smallridge RC *et al.* 2008 Deoxyribonucleic acid profiling analysis of 40 human thyroid cancer cell lines reveals cross-contamination resulting in cell line redundancy and misidentification. *Journal of Clinical Endocrinology and Metabolism* **93** 4331–4341. (doi:10.1210/jc.2008-1102)

Shinohara M, Chung YJ, Saji M & Ringel MD 2007 AKT in thyroid tumorigenesis and progression. *Endocrinology* **148** 942–947. (doi:10.1210/en.2006-0937)

Sounni NE & Noel A 2005 Membrane type-matrix metalloproteinases and tumor progression. *Biochimie* **87** 329–342. (doi:10.1016/j.biochi.2004.07.012)

Stetler-Stevenson WG 2008 Tissue inhibitors of metalloproteinases in cell signaling: metalloproteinase-independent biological activities. *Science Signaling* **1** re6. (doi:10.1126/scisignal.127re6)

Tuyt LM, Dokter WH, Birkenkamp K, Koopmans SB, Lummen C, Kruijer W & Vellenga E 1999 Extracellular-regulated kinase ½, Jun N-terminal kinase, and c-Jun are involved in Nf-κB-dependent IL-6 expression in human monocytes. *Journal of Immunology* **162** 4893–4902.

Vale T, Ngo TT & White MA 2001 Lipsky Raf-induced transformation requires an interleukin 1 autocrine loop. *Cancer Research* **61** 602–607.

Visconti R, Cerutti J, Battista S, Fedele M, Trapasso F, Zeki K, Miano MP, de Nigris F, Casalino L, Curcio F *et al.* 1997 Expression of the neoplastic phenotype by human thyroid carcinoma cell lines requires NF-kB p65 protein expression. *Oncogene* **15** 1987–1994. (doi:10.1038/sj.onc.1201373)

Wan PT, Garnett MJ, Roe SM, Lee S, Niculescu-Duvaz D, Good VM, Jones CM, Marshall CJ, Springer CJ, Barford D *et al.* 2004 Mechanism of activation of the RAF-ER signaling pathway by oncogenic mutations of B-RAF. *Cell* **116** 855–867. (doi:10.1016/S0092-8674(04)00215-6)

Xing M 2007 BRAF mutation in papillary thyroid cancer: pathogenic role, molecular bases and clinical implications. *Endocrine Reviews* **28** 742–762. (doi:10.1210/er.2007-0007)

Yeh MW, Rougier JP, Park JW, Duh QY, Wong M, Werb Z & Clark OH 2006 Differentiated thyroid cancer cell invasion is regulated through epidermal growth factor receptor-dependent activation of matrix metalloproteinase (MMP)-2/gelatinase A. *Endocrine-Related Cancer* **13** 1173–1183. (doi:10.1677/erc.1.01226)

Zhang D, Qiu L, Jin X, Guo Z & Guo C 2009 Nuclear factor-kappaB inhibition by parthenolide potentiates the efficacy of Taxol in non-small cell lung cancer *in vitro* and *in vivo*. *Molecular Cancer Research* **7** 1139–1149. (doi:10.1158/1541-7786.MCR-08-0410)

Received in final form 5 September 2011
Accepted 8 September 2011
Made available online as an Accepted Preprint
8 September 2011